Coherent Beam-Beam Instability in Collisions with a Large Crossing Angle

K. Ohmi,[1,*] N. Kuroo,[1,3] K. Oide,[1,2] D. Zhou,[1,2] and F. Zimmermann[2]
[1]KEK, 1-1 Oho, Tsukuba 305-0801, Japan
[2]CERN, 1211 Geneva 23, Switzerland
[3]University of Tsukuba, Tsukuba, 305-8577, Japan
(Received 14 March 2017; published 26 September 2017)

In recent years the "crab-waist collision" scheme [P. Raimondi, *Proceedings of 2nd SuperB Workshop, Frascati, 2006*.; M. Zobov *et al.*, Phys. Rev. Lett. **104**, 174801 (2010)] has become popular for circular e^+ e^- colliders. The designs of several future colliders are based on this scheme. So far the beam-beam effects for collisions under a large crossing angle with or without crab waist were mostly studied using weak-strong simulations. We present here strong-strong simulations showing a novel strong coherent head-tail instability, which can limit the performance of proposed future colliders. We explain the underlying instability mechanism starting from the "cross-wake force" induced by the beam-beam interaction. Using this beam-beam wake, the beam-beam head tail modes are studied by an eigenmode analysis. The instability may affect all collider designs based on the crab-waist scheme. We suggest an experimental verification at SuperKEKB during its commissioning phase II.

DOI: 10.1103/PhysRevLett.119.134801

Recent and future e^+ e^- colliders adopt a collision scheme with a large horizontal crossing (Piwinski) angle $\sigma_z\theta_c/\sigma_x \gg 1$ [1], where θ_c is the half crossing angle. The vertical beta function is squeezed below the value of the rms bunch length, $\beta_y^* < \sigma_z$, while the crossing angle is chosen as $\sigma_x/\theta_c \leq \beta_y$ to avoid the hourglass effect [2–4]. Crab-waist collision [4,5] achieves a nearly perfect suppression of the hourglass effect for particles with a large horizontal amplitude.

Beam-beam effects for a large-crossing-angle–crab-waist collision were extensively studied using weak-strong simulations. In these simulations a very high beam-beam parameter ($\xi_y > 0.1$) was achieved for the designs of Super B factories [6] and of the e^+ e^- Future Circular Collider (FCC-ee) [7,8]. In a weak-strong simulation one (strong) beam has a fixed charge distribution, so that the incoherent emittance growth of the other (weak) beam can be analyzed. On the other hand, in early 2016 strong-strong simulations revealed a novel coherent beam-beam instability of the head-tail type [9,10]. This instability was observed only when using the strong-strong simulation code "BBSS" [11]. Since the second half of 2016 there has been progress on three fronts: First, another BBSS simulation suggested that this new instability can be experimentally studied at SuperKEKB, during its upcoming phase II of commissioning. Second, it was demonstrated analytically that the cross-wake force induced by beam-beam collisions under a large crossing angle can cause a strong head-tail instability. These two subjects are discussed in the present Letter. Third, D. Shatilov observed the same instability using the code "Lifetrack," based on a quasi-strong-strong model [12,13]. In view of all these findings the instability phenomenon appears to be real. The novel instability may have a strong impact on the design of all future colliders based on large-crossing-angle–crab-waist collision.

The coherent head-tail mode induced by beam-beam interaction without crossing angle has been discussed in Ref. [14]. The head-tail motion was induced by a correlation between the head and tail of a bunch due to a large vertical disruption parameter, $D_y = 2\pi\xi_y\sigma_z/\beta_y$. By contrast, in a collision with a large Piwinski angle, the coherent instability is induced in the horizontal plane, and a strong-strong beam-beam simulation is necessary to study this coherent beam-beam effect. We use the code BBSS, where two colliding bunches are represented by many macroparticles (∼1M) and the collision is modeled via the interactions between the particle distributions. Each bunch is divided into many slices along the longitudinal direction to simulate the collision with a large crossing angle and any resulting head-tail motion. The extension to 3D of the slice-by-slice bunch collision is described in Ref. [15]. Typically the number of slices is chosen as $n_{\rm sl} \approx 10\sigma_z\theta_c/\sigma_x$.

We study the coherent beam-beam instability for SuperKEKB and FCC-ee, considering the parameters of Table I [16]. We first report the instability seen in the simulation, and then present a theoretical explanation based on the beam-beam induced cross-wake force.

Phase I commissioning of SuperKEKB started in February, 2016 without the interaction region (IR) [17]. Beam-beam collision schemes with large crossing angles will be examined in the phase II commissioning that begins in 2018 after installation of the IR. The beta

TABLE I. Parameters for SuperKEKB and FCC-ee.

Parameter		SuperKEKB		FCC-ee-Z		H
		Design	Commissioning	HiLum	Base	
Energy	$E_{+/-}$ (GeV)	4/7		45.5	45.5	120
Bunch population	$N_{+/-}(10^{10})$	9/6.5	6.3/5	10	3.3	8
Emittance	$\varepsilon_{x/y}$ (nm/pm)	3.2/8.64	3.2/44	0.2/1	0.09/1	0.61/1.2
Beta at IP	$\beta^*_{x/y}$ (m/mm)	0.03/0.3	0.25/2.2	0.5/1	1/2	1/2
rms bunch length	σ_z (mm)	6		6.7	3.8	2.4
Energy spread	σ_δ (%)	0.08		0.22	0.09	0.12
Damping time	τ_x/T_0	4000		3000		150
Synchrotron tune	ν_z	0.025		0.036	0.025	0.056
Luminosity per IP	L (10^{34} cm^{-2} s^{-1})	80	⋯	207	90	5.1
Beam-beam parameter	$\xi_{x/y}$	0.0028/0.088	⋯	0.025/0.16	0.05/0.13	0.08/0.14
Piwinski angle	$\sigma_z\theta_c/\sigma_x$	20	8.7	10	6	1.5

functions at the interaction point (IP) will be squeezed sequentially in several steps [18]. The design values are extremely small, $(\beta^*_x, \beta^*_y) = (30, 0.3)$ mm. The phase II target is approximately $(\beta^*_x, \beta^*_y) = (240, 2.4)$ or (120, 2.4) mm, that is, they are $(8\times, 8\times)$ and $(4\times, 8\times)$ of the design, respectively.

A strong-strong simulation was performed using these β^* values. The beam-beam parameter, calculated as normalized luminosity, i.e., $\xi_L = 2r_e\beta_y L/(N_e\gamma f_{\rm rep})$, is used as an indicator of the beam-beam limit.

No unstable behavior was seen for the SuperKEKB design parameters with very small β^*_{xy} [19]. We, therefore, focus on the commissioning stage. Figures 1(a) and 1(b) show the beam-beam parameter and head-tail motion $\langle xz\rangle$, respectively, for β^* enhanced $(8\times, 8\times)$ and $(4\times, 8\times)$. Simulations were performed with and without the crab waist [CW (NoCW)]. A strong coherent beam-beam instability is seen with $(8\times, 8\times)$, but not with $(4\times, 8\times)$. This difference of $(8\times, 8\times)$ and $(4\times, 8\times)$ can be observed in the SuperKEKB commissioning. The crab waist is not a primary reason for the instability, but it has an effect on the luminosity.

The design of the FCC-ee-H aims for a beam-beam parameter of $\xi_y \sim \xi_L = 0.14$/IP. Because the FCC-ee has two IPs, we used a half ring model with 50 km circumference and doubled the dimensionless damping time in the simulation. The Piwinski angle (PA) is $\sigma_z\theta_c/\sigma_x = 1.5$ in the design. The simulation is performed for the half crossing angles $\theta_c = 0.015$ and 0.02 rad (PA $= \sigma_z\theta_c/\sigma_x = 1.5$ and 2) to investigate the effects of the Piwinski angle. The tune operating point for the half ring is $(\nu_x, \nu_y) = (0.54, 0.61)$, which has been optimized by weak-strong simulations [20,21].

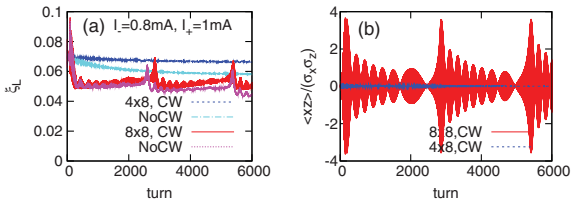

FIG. 1. Strong-strong simulation results for SuperKEKB. (a) and (b) show the beam-beam parameter and head-tail motion $\langle xz\rangle$, respectively, at the commissioning stage with IP beta, $(8\times, 8\times)$, and $(4\times, 8\times)$.

Figure 2 presents the simulation results for the FCC-ee-H. Figures 2(a) and 2(b) show the evolution of the beam-beam parameter for $\sigma_z\theta_c/\sigma_x = 1.5$ and 2, respectively. Bunch populations of 4–16 $\times$ 10^{10} are examined, while the design value is 8×10^{10}. The coherent motion of $\langle xz\rangle$ is not seen for PA $= 1.5$, but it is observed for PA $= 2$. Figure 2(c) shows a summary of the equilibrium beam-beam parameters. The error bars depict the fluctuations due to coherent motion. The beam-beam parameter is saturated at approximately

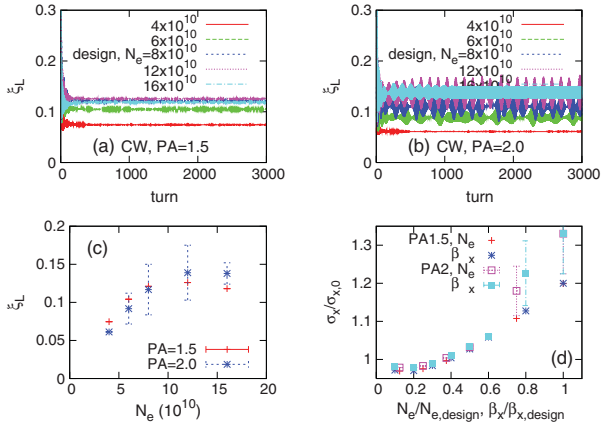

FIG. 2. Beam-beam simulation results for FCC-ee-H obtained by the full PIC strong-strong method. The evolutions of the beam-beam parameter for PA $= 1.5$ and 2 are shown in (a) and (b), respectively. The final beam-beam parameters as a function of bunch population (N_e) and the stationary horizontal beam size as functions of N_e and β^*_x are summarized in (c) and (d), respectively.

0.12 in both PA = 1.5 and 2, independently of the occurrence of coherent instability. The value of β_x^* is the key parameter for the coherent instability in SuperKEKB. Simulations for various values of β_x^* were performed, while keeping the horizontal beam size at the IP constant (by adjusting the horizontal emittance). Figure 2(d) shows the stationary horizontal beam size for various values of $N_\pm$ and β_x^*. The stationary beam size depends on the product $N_\pm\beta_x^*$. At the design β_x^*, the beam size increases for $N_\pm \geq 2$–3×10^{10} [$N/N_{\rm design} \geq 0.25$ in Fig. 2(d)], which is taken to be the threshold of an instability. Indeed, a coherent excitation of the second moment $\langle xz \rangle$ in the early stage of the simulation seems to be the cause of this beam size increase. Following the beam size increase the coherent motion disappears for PA = 1.5, and also for PA = 2, up to a second threshold. For PA = 2, at higher bunch intensities of $N_\pm \geq 6 \times 10^{10}$, the coherent motion persists even after, or with, the beam size increase.

The FCC-ee Z factory is designed with a larger Piwinski angle of PA = 6 or 10. The target beam-beam parameter is 0.13 or 0.16, for PA = 6 or 10, respectively. The tune operating point for the half ring is $(\nu_x, \nu_y) = (0.54, 0.61)$.

The coherent motion in $\langle xz \rangle$ is seen even at low current, where the thresholds are $N_\pm = 1.3 \times 10^{10}$ (40% of the design) and 3×10^{10} (30% of the design) for PA = 6 and 10, respectively. Figure 3 presents the simulation results for FCC-ee-Z. Figure 3(a) displays the beam-beam parameter as a function of the bunch population. The error bars depict the fluctuation in luminosity. The beam-beam parameter saturates at 0.1 and 0.04 at PA = 6 and 10, respectively. The limit value $\xi_L = 0.04$ at PA = 10 is very low. The coherent instability is more serious for larger Piwinski angles.

Figure 3(b) shows the beam-beam parameter as a function of β_x^*. We hold the horizontal IP beam size constant, and consider the design bunch population. The coherent instability and luminosity fluctuation disappear at $\beta_x^* \leq 0.08$ m for both PA = 6 and 10. The luminosity or beam-beam parameters recover their design values of 0.12 and 0.15 for PA = 6 and 10, respectively, at $\beta_x^* \leq 0.08$ m.

The two bunch tilts $\langle xz \rangle$ of the unstable e^+ and e^- beams always oscillate in phase, for SuperKEKB, FCCee-H, and Z; i.e., in all cases coherent beam-beam instability occurs for the head-tail "σ" mode.

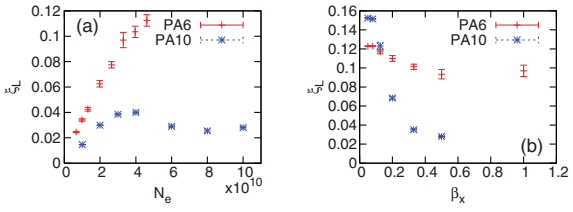

FIG. 3. Simulation results for FCC-ee-Z. (a) the beam-beam parameter as a function of the bunch population, (b) the beam-beam parameter as a function of β_x^*.

For an understanding of the coherent instability, we introduce a cross-wake force caused by the beam-beam interaction. The cross-wake force mediates the correlation between two colliding bunches. Figure 4(a) illustrates how we evaluate the wake force. Namely, we consider two bunches tilted by half crossing angle in the x-s plane which collide with each other by moving in the opposite s direction. Without any translational motion in the x direction, for longitudinal position $z_\pm$ the horizontal position of the bunch center is $x_\pm = \theta_c z_\pm$. We assume a deviation of Δx_- in part of the e^- bunch. A part of the e^+ bunch with z_+ interacts with the part of the e^- bunch with equal s, $s = (z_+ - z_-)/2$. The perturbed momentum kick of that part of the e^+ bunch is expressed by

$$\Delta p_x^{(+)} = -\frac{n_- r_e}{\gamma_+}[F_x(x_+ - x_- - \Delta x_-) - F_x(x_+ - x_-)], \quad (1)$$

where F_x is given by the Bassetti-Erskine formula [22] with asymptotic form $F_x \to 2/x$ for large x. n_- is the number of electrons contained in the associated part of the e^- bunch. The momentum kick for the static case, i.e., without any deviation of the e^- bunch, is subtracted. For a flat beam, F_x only weakly depends on $y \approx O(\sigma_y)$. The momentum kick $\Delta p_x^{(+)} = -W_x^{(+)}(z_+ - z_-)\rho_x^{(-)}\Delta z_-$ is represented through a "cross-wake" force $W^{(+)}$ as

$$W_x^{(+)}(z_+ - z_-) = -\frac{N_- r_e}{\gamma_+}\frac{\partial F_x}{\partial x}\bigg|_{x=(z_+-z_-)\theta_c}. \quad (2)$$

The wake force W_x is shown in Fig. 4(b). Above, $\rho_x^{(-)}(z)$ is the longitudinal density distribution of the horizontal dipole moment. An important relation links horizontal and longitudinal displacements: $n_-\Delta x_- = N_-\rho_x^{(-)}\Delta z_-$. The momentum kick is obtained by integrating over the dipole moment density of the opposite bunch:

$$\Delta p_{x,\pm}(z_\pm) = -\int_{-l}^{l} W_x^{(\pm)}(z_\pm - z'_\mp)\rho_x^{(\mp)}(z'_\mp)dz'_\mp. \quad (3)$$

The minimum cross wake is $W_x^{(\pm)}(0) \approx -N_\mp r_e/(\gamma_\pm\sigma_x^2)$ at $z = 0$, where $\sigma_x^2 = (\sigma_{x+}^2 + \sigma_{x,-}^2)/2$.

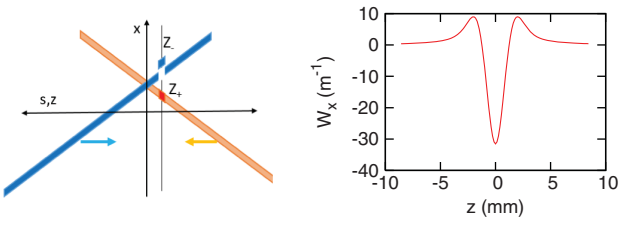

FIG. 4. (a) Illustration of the evaluation of the wake force induced by the beam-beam interaction. and (b) obtained wake force for FCC-ee-Z (PA = 10).

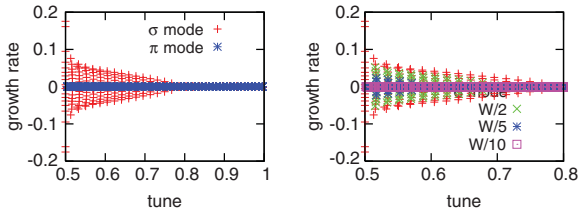

FIG. 5. Growth rate for each eigenmode [FCC-ee-Z (PA = 10)] as a function of the eigenmode tune, for a bare tune $\nu_x = 0.54$.

We consider the σ mode, in which dipole moments are equal, $\rho_x^{(+)}(z) = \rho_x^{(-)}(z)$, and the π mode, in which they are opposite $[\rho_x^{(+)}(z) = -\rho_x^{(-)}(z)]$, where the transparency conditions $N_+\gamma_+ = N_-\gamma_-$, $\sigma_{+,xyz} = \sigma_{-,xyz}$ $\nu_{+,xyz} = \nu_{-,xyz}$ are assumed. Equation (3) then reduces to the usual formula for the wake force of a single bunch,

$$\Delta p_x(z) = \mp \int_{-l}^{l} W_x(z - z')\rho_x(z')dz, \tag{4}$$

where the $-(+)$ sign is chosen for $\sigma(\pi)$ modes, respectively.

A mode analysis for the horizontal dipole moment can now be carried out in longitudinal phase, using

$$x_{ij} = x(J_i, \phi_j), \quad p_{ij} = p_x(J_i, \phi_j), \quad \psi_i = \psi(J_i), \tag{5}$$

where ψ is the density distribution in longitudinal phase space, $\psi = \exp(-J/\varepsilon_z)/(2\pi\varepsilon_z)$. The longitudinal phase space is discretized as [23]

$$J_i^{1/2} = i\Delta J^{1/2}, \quad \phi_j = 2\pi\nu_s j, \quad z_{ij} = \sqrt{2\beta_z J_i}\cos\phi_j, \tag{6}$$

where $i = 1,\ n_J,\ j = 1,\ 1/\nu_s$. For simplicity $1/\nu_s$ is assumed to be an integer. Effects of synchro-betatron resonances are determined by the relation between synchrotron and betatron tunes, and our assumption for $1/\nu_s$ does not constrain this relation. For one arc revolution, the transverse betatron oscillation is modeled by a matrix transformation for (x_{ij}, p_{ij}), as

$$M_0 = \delta_{i,i'}\delta_{j-1,j'}\begin{pmatrix} \cos 2\pi\nu_x & \sin 2\pi\nu_x \\ -\sin 2\pi\nu_x & \cos 2\pi\nu_x \end{pmatrix}, \tag{7}$$

where $\nu_x = 0.54$. The synchrotron motion is represented by transforming with the Kronecker delta, $\delta_{j-1,j'}$. The transformation for the momentum kick due to the wake force is expressed by

$$M_W = \begin{pmatrix} \delta_{i,i'}\delta_{j,j'} & 0 \\ -\beta_x W(z_{i,j} - z_{i',j'})\psi_{i'}\Delta J\Delta\phi & \delta_{i,i'}\delta_{j,j'} \end{pmatrix}. \tag{8}$$

Stability of the colliding bunches is discussed by eigenvalues/vectors of the matrix product $M_W M_0$, where the size of matrices is $(2 \times n_J \times 1/\nu_s)^2$. $n_J = 40$, $\Delta J^{1/2} = 0.05\varepsilon_z^{1/2}$, $1/\nu_s = 56$ are chosen for FCCee-Z (PA = 10). The size of matrices is 4480^2. Eigenvalues (λ's) are plotted in Fig. 5, where the growth rate per revolution and tune are given by $\log|\lambda|$ and $\tan^{-1}(\mathrm{Im}\lambda/\mathrm{Re}\lambda)/(2\pi)$, respectively. Figure 5(a) shows the growth rate for σ/π modes. All of the π modes are stable. Pairs of growth and damping modes are seen in the σ modes. The unstable tunes are $0.5 + m\nu_s$, $m \leq 14$. The most unstable mode is at $\nu = 0.5$. Figure 5(b) shows the growth rate for changing strengths of the wake force: 1/2, 1/5, and 1/10 of the nominal. The unstable modes disappear at 1/10. This instability is a phenomenon with a threshold.

TABLE II. Threshold bunch intensities in units of 10^{10} obtained using three different approaches.

Collider	BBSS	Mode analysis	Tracking
FCC-ee-Z HiLum	2–3	1.2	1.2
FCC-ee-H	2–3	2.3	2.1

We also performed particle tracking simulations of two bunches or a single bunch modeling the collision with the cross-wakes of Eqs. (3) and (4), respectively, and the rest of the ring by a simple revolution matrix, using self-developed programs in FORTRAN or C++, and considering 10 000 macroparticles per bunch. A numerical comparison of instability thresholds obtained by the three different methods is presented in Table II.

In conclusion, we studied coherent beam-beam effects with a large Piwinski angle and crab-waist collision using a strong-strong simulation code, BBSS. Simulations for SuperKEKB, FCC-ee-H, and FCC-ee-Z show a strong coherent beam-beam instability in the head-tail σ mode. The coherent instability is of an acceptable magnitude for the SuperKEKB design parameters and for FCC-ee-H, but it is serious for FCC-ee-Z. The existence and threshold of this instability can be experimentally verified during the SuperKEKB commissioning with a relaxed β_x^* (which is presently scheduled for the spring of 2018). Squeezing β_x^* helps mitigate the instability. As a result of our study, the base line parameters of the FCC-ee-Z have been changed to $\beta_x^* = 0.15$–0.2 m and $\varepsilon_x = 260$ pm [13]. A theoretical model based on the beam-beam wake force can explain this instability. The associated mode-coupling analysis reveals unstable head-tail σ modes. Controlling this instability is essential for the design of future lepton colliders, such as FCC [24], CEPC [25], BINP charm-tau [26], SuperKEKB [17], etc.

The authors thank Dr. Y. Cai, Dr. D. Shatilov, Dr. Y. Zhang, and Dr. M. Benedikt for fruitful discussions. They also thank Dr. J. Flanagan and Dr. E. Forest for reading the manuscript. This research project was supported, in part, by the European Commission's Horizon 2020 Programme through the Marie S.-Curie RISE project E-Jade, Contract No. 645479, and the IA project ARIES, Grant No. 730871.

*kazuhito.ohmi@kek.jp

[1] A. Piwinski, DESY Report No. DESY 77/18, 1977.
[2] K. Hirata, Phys. Rev. Lett. **74**, 2228 (1995).
[3] F. Ruggiero and F. Zimmermann, Phys. Rev. ST Accel. Beams **5**, 061001 (2002).
[4] P. Raimondi, D. Shatilov, M. Zobov, *Proceedings of 2nd SuperB Workshop, Frascati, 2006* [arXiv:physics/0702033], LNF-07-003-IR.
[5] M. Zobov *et al.*, Phys. Rev. Lett. **104**, 174801 (2010).
[6] D. Shatilov, E. Levichev, E. Simonov, and M. Zobov, Phys. Rev. ST Accel. Beams **14**, 014001 (2011).
[7] A. Bogomyagkov, E. Levichev, and D. Shatilov, Phys. Rev. ST Accel. Beams **17**, 041004 (2014).
[8] K. Ohmi and F. Zimmermann, Proceedings of IPAC14, Dresden, Germany (2014), THPRI004.
[9] K. Ohmi, Int. J. Mod. Phys. A, **31**, 1644014 (2016).
[10] K. Ohmi, *Proceedings of IPAC16, Busan, Korea* (2016), MOZA01.
[11] K. Ohmi, Phys. Rev. E **62**, 7287 (2000).
[12] See https://indico.cern.ch/event/615842/.
[13] See https://indico.cern.ch/event/617116/.
[14] E. A. Perevedentsev and A. A. Valishev, Phys. Rev. ST Accel. Beams **4**, 024403 (2001).
[15] K. Ohmi, M. Tawada, Y. Cai, S. Kamada, K. Oide, and J. Qiang, Phys. Rev. ST Accel. Beams **7**, 104401 (2004).
[16] K. Oide *et al.*, Phys. Rev. Accel. Beams **19**, 111005 (2016).
[17] H. Koiso, *Proceedings of IPAC17, Copenhagen, Denmark* (2017), TUZB2; See http://www-superkekb.kek.jp/.
[18] Y. Funakoshi, Proceedings of eeFACT16, 2016 (Cockcroft Inst., UK, 2016).
[19] K. Ohmi, *Proceedings of IPAC11, San Sebastian, Spain* (2011), p. 3697.
[20] Y. Zhang, K. Ohmi, and D. Shatilov, *Proceedings of IPAC14, Dresden, Germany* (2014), THPRI003, p. 3763.
[21] D. Zhou, H. Koiso, A. Morita, K. Ohmi, Y. Ohnishi, K. Oide, and H. Sugimoto, *Proceedings of IPAC15, Richmond, VA, USA* (2015), p. 2413.
[22] M. Bassetti and G. Erskine, Report No. CERN ISR TH/80-06, 1980.
[23] K. Oide, Part. Accel. **51**, 43 (1995).
[24] See https://indico.cern.ch/event/556692/.
[25] See http://cepc.ihep.ac.cn/.
[26] See https://ctd.inp.nsk.su/c-tau/.